Inorg. Chem. **2006**, *45*, 4364–4371

Intercalation and Photophysical Properties of the Tetra-(8-hydroxyquinolinato) Boron Complex and 3,3′,4,4′-Benzophenone Tetracarboxylic Anion into Mg–Al Layered Double Hydroxides

Zhong-Liang Wang,[†] Zhen-Hui Kang,[†] En-Bo Wang,*[,†] Zhong-Min Su,*[,‡] and Lin Xu[†]

Institute of Polyoxometalate Chemistry, Department of Chemistry, Northeast Normal University, Changchun, Jilin 130024, P.R. China and Institute of Functional Materials, Department of Chemistry, Northeast Normal University, Changchun, Jilin, 130024 P.R. China

Received November 17, 2005

The tetra-(8-hydroxyquinolinato) boron complex (Bq) and 3,3′,4,4′-benzophenone tetracarboxylic anion (BPTC) were successfully intercalated into layered double hydroxides with an ion-exchange method. Elemental analyses, powder X-ray diffraction, FTIR spectra, and thermogravimetric analyses indicated that the hydrothermal treatment could efficiently improve the reaction process, the purity and crystallinity of products, and that Bq and BPTC molecules steadily arranged with C2 axis perpendicular to the layer plane, and the J-type aggregate in the host interlayer, respectively. The fluorescence studies showed that, compared with those observed in the dilute solutions of the guests, the spectra of Mg_3Al–Bq and Mg_3Al–BPTC evolved to the high-energy side and the low-energy side with increasing their loading, respectively, which were attributed to various arrangements of guests and the increased intermolecular interaction. Furthermore, their fluorescence intensity gradually decreased with increasing the intercalated guest content due to the concentration quenching, and Mg_3Al–Bq exhibits enhanced solid-state blue luminescence due to a more rigid and constrained environment of the host.

Introduction

The design, synthesis, and properties of multifunctional materials are a topic of great interest that involve solid-state and materials chemistry.[1,2] The introduction of hybrid strategy provides a promising way of producing innovative inorganic−organic functional materials with ordered nanostructure and tailored properties.[3−5] It should be pointed out that these properties generally differ from those of the pure guest species, being affected by host−guest interaction, affecting the distribution and orientation of guest in the host, and guest−guest interaction, responsible for the guest aggregate (H-type or J-type aggregates).[6−8] Indeed, encapsulations of some cationic dyes or cationic photoactive species into inorganic host system, such as zeolites and cationic clays, to construct novel photofunctional materials, have been extensively investigated.[9−11] This can not only improve the photophysical and photochemical properties of the guest, but also increases the thermal- and photostability of the guest. However, the majority of photoactive species are anionic and cannot be intercalated into cationic host matrix.

Recently, the combination of two-dimension layered solids and intercalation techniques offer a new area for developing new hybrids with desired functionality.[12] Among the layered solids, layered double hydroxides (LDHs), also known as anionic clays, occupy a unique place not only due to their rich intercalation chemistry but also because of synergistic and complementary features, as well as extensive applications

* To whom correspondence should be addressed. E-mail: wangenbo@public.cc.jl.cn.

[†] Institute of Polyoxometalate Chemistry, Department of Chemistry, Northeast Normal University, Fax: +86-431-5098787.

[‡] Institute of Functional Materials, Department of Chemistry, Northeast Normal University.

(1) Mueller, A.; Reuter, H.; Dillinger, S. *Angew. Chem., Int. Ed. Engl.* **1995**, *34*, 2328.
(2) Ferey, G. *J. Solid State Chem.* **2000**, *152*, 37.
(3) Ozin, G. A. *Adv. Mater.* **1992**, *4*, 612.
(4) Ellerby, L. M.; Nishida, C. R.; Nishida, F.; Yamanaka, S. A.; Dunn, B.; Valentine, J. S.; Zink, J. I. *Science* **1992**, *255*, 1113.
(5) Gomez-Romero, P. *Adv. Mater.* **2001**, *13*, 163.
(6) Ogawa, M.; Kuroda, K. *Bull. Chem. Soc. Jpn.* **1997**, *70*, 2593.
(7) Schulz-Ekloff, G.; Wöhrle, D.; Van Duffe, B.; Schoonheydt, R. A. *Microporous Mesoporous Mater.* **2002**, *51*, 91.
(8) Martínez, V. M.; Arbeloa, F. L.; Prieto, J. B.; Arbeloa, I. L. *J. Phys. Chem. B* **2005**, *109*, 7443.
(9) Thomas, J. K. *Acc. Chem. Res.* **1988**, *21*, 275.
(10) Ogawa, M.; Kuroda, K. *Chem. Rev.* **1995**, *95*, 399.
(11) Calzaferri, G.; Huber, S.; Maas, H.; Minkowski, C. *Angew. Chem., Int. Ed.* **2003**, *42*, 3732.
(12) Choy, J.-H.; Kwon, S. J.; Park, G. S. *Science* **1998**, *280*, 1589.

10.1021/ic0519887 CCC: $33.50
Published on Web 04/28/2006

in catalysis, adsorption, separation, medical science, and functional materials,[13−21] which make LDHs rare examples of layered solids with positively charged layers balanced by exchangeable anions. However, LDHs are still experiencing slow development of the photofunctional materials in spite of the important role that the host matrix may play in confining guest in restrained environment and modulating their optical properties. Recently, a few published remarkable works[22−28] have focused on the incorporation or photochemical properties of chromophores in the interlayer of Mg−Al and Zn−Al LDHs, and the recent work of Costantino et al.[29−31] in alignment of dyes within the host interlayer that exhibit the considerable red-shift of fluorescence spectra compared with that in the dilute solution is also a good example. These above not only confirm the feasibility to fabrication of the optical materials with LDHs and the chromophore anions but also bring a beneficial pathway to further develop such electronic and optical materials.

In the present paper, tetra-(8-hydroxy-quinolinato) boron (Bq) complex with a tetrahedral-like geometry and 3,3′,4,4′-benzophenone tetracarboxylic (BPTC) anion with a long-chain structure that can compensate for the positive charge of the LDHs layers has first been employed to construct the new photofunctional materials, Mg_3Al-Bq and $Mg_3Al-BPTC$, respectively, not only because of their various orientations in the host interlayer, which have significant effect on the photophysical properties, but also because of their important applications in the fabrication of devices[32−35] and the photochemistry reaction,[36−38] respectively. In particular, relatively few studies have been devoted to photophysical properties of those anions adsorbed on a solid surface,[39−42] although such studies may be important for understanding the optoelectronic properties and the mechanistic organic photochemistry on a molecular level. The studies indicate that Bq and BPTC molecules steadily arranged with a C2 axis perpendicular to the host layers and the J-type aggregate in the host interlayer, respectively, and that Mg_3Al-Bq and $Mg_3Al-BPTC$ possess guests' orientation and loading dependencies of the excitation and emission spectra due to the formation of the various aggregates and the increased intermolecular interaction. Furthermore, to the best of our knowledge, it is the first report that their fluorescence intensity can be finely controlled by varying the guest loading and that Mg_3Al-Bq exhibits enhanced solid-state blue luminescence due to a more rigid and confined environment of the host.

Experimental Section

All chemicals were commercially purchased and used without further purification. Element analyses were performed in the Vernaison Analysis Center of CNRS by inductively coupled plasma-atomic emission spectrometry (ICP-AES). The PXRD analysis was conducted using a Rigaku D/max-IIB X-ray diffractometer at a scanning rate of 4° min^{-1}, using Cu Kα radiation ($\lambda = 1.5418$ Å); all samples were dried in a vacuum desiccator at 80 °C to compare. Fourier transform infrared spectra were recorded using a Perkin-Elmer model 1725X spectrophotometer in the range 400−4000 cm^{-1}, and the standard KBr disk method was used. Thermogravimetric analysis (TGA) curves were recorded under airflow at a heating rate of 10 °C min^{-1}. Fluorescence spectra corrected for the instrumental response were recorded on a SPEX Fluorolog-2T2 spectrofluorometer equipped with a 450-W xenon lamp as the excitation source at room temperature.

Sample Preparation. $Na[B(C_9H_6ON)_4]$ (Bq complex) was prepared according to the literature method.[34] To a suspension of sodium borohydride (0.76 g, 0.02 mol) in absolute ethanol (20 mL) was added a solution of 8-hydroxyquinoline (11.6 g, 0.08 mol) in absolute ethanol (120 mL) dropwise with magnetic stirring. A precipitate formed immediately, and stirring was continued for 2 h after all of 8-hydroxyquinoline have been added. The precipitate was filtered, purified with ethyl ether, and dried under vacuum to yield white powder. The yield is about 91%. Elemental anal. (%) for $C_{36}H_{24}N_4O_4BNa$, Calcd: C 70.82, H 3.93, N 9.18, Na 3.77; Found: C 70.68, H 4.06, N 9.05, Na 3.47.

The Mg_3Al-Cl was prepared with a coprecipitation method. Typically, a mixed solution of 1 M $MgCl_2$ and 1 M $AlCl_3$ (Mg/Al ratio = 3) was added dropwise to a 4 M NaOH solution under

(13) Cavani, F.; Trifiro, F.; Vaccari, A. *Catal. Today* **1991**, *11*, 173.
(14) Newman, S. P.; Jones, W. *New J. Chem.* **1998**, *22*, 105, and references therein.
(15) Hu, C. W.; He, Q. L.; Zhang, Y. H.; Zhang, Y. H.; Liu, Y. Y.; Zhang, Y. F.; Tang, T. D.; Zhang, J. Y.; Wang, E. B. *Chem. Commun.* **1996**, 121.
(16) Rives, V. In *Layered Double Hydroxides: Present and Future*; Rives, V., Ed.; Nova Science Publications: New York, 2001.
(17) Choy, J.-H.; Kwak, S.-Y.; Jeong, Y.-J.; Park, J.-S. *Angew. Chem., Int. Ed.* **2000**, *39*, 4041.
(18) Khan, A. I.; Lei, L. X.; Norquist, A. J.; O'Hare, D. *Chem. Commun.* **2001**, 2342.
(19) Wang, Z. L.; Wang, E. B.; Gao, L.; Xu, L. *J. Solid State Chem.* **2005**, *178*, 736.
(20) Leroux, F.; Besse, J.-P. *Chem. Mater.* **2001**, *13*, 3507.
(21) Liu, J.-J.; Li, F.; Evans, D. G.; Duan, X. *Chem. Commun.* **2003**, 542.
(22) Giannelis, E. P.; Nocera, D. G.; Pinnavaia, T. J. *Inorg. Chem.* **1987**, *26*, 203.
(23) Park, I. Y.; Kuroda, K.; Kato, C. *J. Chem. Soc., Dalton Trans.* **1990**, 3071.
(24) Tagaya, H.; Ogata, A.; Kuwahara, T.; Ogata, S.; Karasu, M.; Kadokawa, J.; Chiba, K. *Microporous Mater.* **1996**, *7*, 151.
(25) Bonnet, S.; Forano, C.; de Roy, A.; Besse, J. P.; Maillard, P.; Momenteau, M. *Chem. Mater.* **1996**, *8*, 1962.
(26) Bauer, J.; Behrens, P.; Speckbacher, M.; Langhals, H. *Adv. Funct. Mater.* **2003**, *13*, 241.
(27) Takagi, K.; Shichi, T.; Usami, H.; Sawaki, Y. *J. Am. Chem. Soc.* **1993**, *115*, 4339.
(28) Tagaya, H.; Kuwahara, T.; Sato, S.; Kadokawa, J.; Karasu, M.; Chiba, K. *J. Mater. Chem.* **1993**, *3*, 317.
(29) Costantino, U.; Colitti, N.; Nocchetti, M.; Aloisi, G. G.; Alisei, F. *Langmuir* **1999**, *15*, 4454.
(30) Costantino, U.; Colitti, N.; Nocchetti, M.; Aloisi, G. G.; Alisei, F.; Latterini, L. *Langmuir* **2000**, *16*, 10351.
(31) Costantino, U.; Nocchetti, M. In *Layered Double Hydroxides: Present and Future*; Rives, V., Ed.; Nova Science Publications: New York, 2001; Chapter 12.
(32) Tang, C. W.; Vanslyke, S. A.; Chen, C. H. *Appl. Phys. Lett.* **1987**, *51*, 913.
(33) Hamada, Y. *IEEE Trans. Electron Devices* **1997**, *44*, 1206.
(34) Tao, X. T.; Suzuki, H.; Wada, T.; Miyata, S.; Sasabe, H. *J. Am. Chem. Soc.* **1999**, *121*, 9447.
(35) Kumar, L.; Koireng, R. R.; Misra, A.; Kumar, P.; Dhawan, S. K.; Kamalasanan, M. N.; Chandra, S. *Ind. J. Pure Appl. Phys.* **2005**, *43*, 56.
(36) Shimada, R.; Goodman, L. *J. Chem. Phys.* **1965**, *43*, 2027.
(37) Lamola, A. A. *J. Chem. Phys.* **1967**, *47*, 4810.
(38) Turro, N. J. *Modern Molecular photochemistry*; University Science Books: Mill Valley, CA, 1991.
(39) Cizmeciyan, D.; Sonnichsen, L. R.; Garcia-Garibay, M. A. *J. Am. Chem. Soc.* **1997**, *119*, 184.
(40) Corrent, S.; Martinez, L. J.; Scaiano, J.; Garcia, H.; Fornes, V. *J. Phys. Chem. B* **1999**, *103*, 8097.
(41) Thomas, J. K. *Photochem. Photobiol. Sci.* **2004**, *3*, 483.
(42) Nishiguchi, H.; Zhang, J.-L.; Anpo, M. *Langmuir* **2001**, *17*, 3958.

vigorous stirring, and the pH was then adjusted with 1 M NaOH to 10 ± 0.3. The gel-like mixture was aged at 65 °C for 18 h. Upon cooling, the product was separated by filtration until most of the water had been removed; the filter cake was not allowed to dry. The product was washed by reslurrying with fresh deionized water and stored in a 500 mL jar.

Here, the classic ion-exchange method was successfully adopted and the hydrothermal technique, occupying a unique place in modern science and technology, is used. Recent studies also verify that mild hydrothermal processes can improve the rate of reaction and the crystallinity of products.[43−45]

Mg_3Al−Bq. To a 25 mL portion of the preceding Mg_3Al−Cl slurry (2.5 mmol) with pH (6−7) adjusted by 1 M HCl aqueous solution was dropwisely added a solution consisting of the Bq in the mixed solvent of deionized water and acetone with vigorous stirring and continued stirring for 30 min under a blanket of N_2. The mixture was sealed in a 50 mL Teflon-lined autoclave and heated at 110 °C for 3 days. Then the autoclave was cooled to room temperature, the precipitates obtained were filtered, washed repeatingly with ethanol, acetone, and water, and dried in a vacuum desiccator overnight. The loading of the Bq was controlled by the concentration of the Bq solution.

Mg_3Al−BPTC. To a 25 mL portion of the preceding Mg_3Al−Cl slurry (2.5 mmol) with pH (5−6) adjusted by 1 M HCl aqueous solution was added dropwise an aqueous solution of the BPTC at vigorous stirring and continued stirring for 30 min under a blanket of N_2. The mixture was sealed in a 50 mL Teflon-lined autoclave and heated at 110 °C for 2 days; then the autoclave was cooled to room temperature. The starting BPTC/LDHs mole ratio was changed from 0 to 0.8. When the aging pattern for the high concentration of the BPTC solution was changed, the product was obtained at 60 °C. All the precipitates obtained were filtered, washed repeatedly with deionized water, and dried in a vacuum desiccator overnight. The experiments were actually carried out in the N_2 atmosphere.

Results and Discussion

Structural and Compositional Analysis. PXRD patterns of the two samples of Mg_3Al−BPTC prepared by two different aging conditions (110 °C under hydrothermal treatment and 60 °C) are given in Figure 1. Only hydrothermal treatment can yield the pure and well-crystallized Mg_3Al−BPTC with an average basal spacing of 12.60 Å. In contrast, partly exchanged product is obtained without hydrothermal condition and exhibits a new series of broader reflections due to poor crystallinity, even if the exchange at various temperatures from 60 up to 110 °C during 4 days does not ameliorate the purity and crystallinity of products. These indicate that the BPTC molecules do not exchange as easily as the other alkanediate anions, probably because of the complexing power of BPTC anions, which react spontaneously with metallic cations and oxides, impeding the intercalation.[46,47] Thus, high BPTC concentrations and the hydrothermal treatment are needed to shift the equilibrium, which then gives the pure and well-crystallized products.

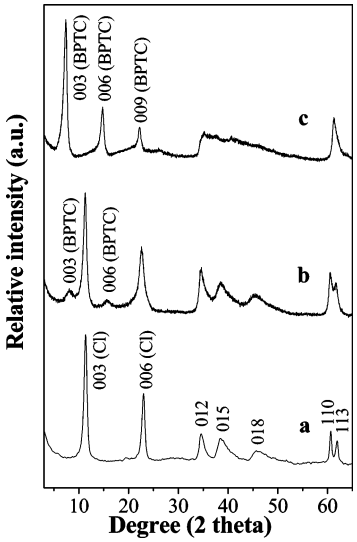

Figure 1. PXRD patterns for the Mg_3Al−Cl precursor (a) and the intercalates obtained at the starting BPTC/LDHs mole ratio, 0.8, with the various aging treatment at (b) 60 and (c) 110 °C under hydrothermal condition.

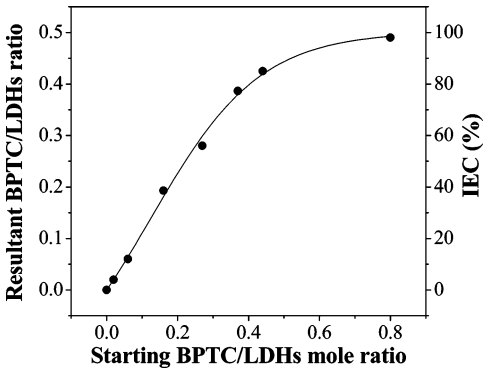

Figure 2. BPTC uptake of LDHs as a function of the starting BPTC/LDHs mole ratio. Here, the BPTC/LDHs ratio indicates the mole ratio of BPTC to Al in LDHs.

Figure 2 reports the incorporation of BPTC anions into the LDHs, under hydrothermal treatment at 110 °C, as a function of the starting BPTC/LDHs mole ratios, indicating that the starting ratio and resultant ratio are different and that only about 50% of the starting BPTC molecules is incorporated into the interlayer space. Chemical compositions of obtained compounds Mg_3Al−BPTC and Mg_3Al−Cl are given in Table 1. The ratio of divalent to trivalent metal of the synthesized precursors conforms well to the expected ratio, indicating that both divalent and trivalent metal quantitatively precipitated during the coprecipitation processes. (note: according to the elemental analysis, each BPTC anion bears two units of negative charges because of protonization with two H^+ under the acid condition; further verification sees anion packing). After the ion-exchange reaction, M^{II}/M^{III} molar ratios of Mg_3Al−BPTC show a minor change due to a partial dissolution of the divalent ion of the layers under hydrothermal synthesis. This is another indication that the interlamellar anion concentration can be finely controlled by the ion-exchange method. As

(43) Kooli, F.; Rives, V.; Ulibarri, M. A. *Inorg. Chem.* **1995**, *34*, 5114.
(44) Tronto, J.; dos Reis, M. J.; Silvério, F.; Balbo, V. R.; Marchetti, J. M.; Valim, J. B. *J. Phys. Chem. Solids* **2004**, *65*, 475.
(45) Beaudot, P.; De Roy, M. E.; Besse, J. P. *Chem. Mater.* **2004**, *16*, 935.
(46) Pisson, J.; Taviot-Guého, C.; Israëli, Y.; Leroux, F.; Munsch, P.; Itié, J.-P.; Briois, V.; Morel-Desrosiers, N.; Besse, J.-P. *J. Phys. Chem. B* **2003**, *107*, 9243.
(47) Iyi, N.; Kurashima, K.; Fujita, T. *Chem. Mater.* **2002**, *14*, 583.

Table 1. Chemical Compositions for the LDH Intercalates

sample (IEC)	M^{II}/M^{III} ratio	proposed formulas
Mg_3AlCl	3.0	$Mg_{0.75}Al_{0.25}(OH)_2(Cl)_{0.250}\cdot 1.0H_2O$
$Mg_3AlBPTC$ (4%)	3.0	$Mg_{0.75}Al_{0.25}(OH)_2(BPTC)_{0.010}(Cl)_{0.230}\cdot 0.9H_2O$
$Mg_3AlBPTC$ (12%)	3.0	$Mg_{0.75}Al_{0.25}(OH)_2(BPTC)_{0.030}(Cl)_{0.190}\cdot 0.9H_2O$
$Mg_3AlBPTC$ (38%)	2.9	$Mg_{0.75}Al_{0.26}(OH)_2(BPTC)_{0.077}(Cl)_{0.126}\cdot 1.0H_2O$
$Mg_3AlBPTC$ (56%)	2.8	$Mg_{0.74}Al_{0.26}(OH)_2(BPTC)_{0.101}(Cl)_{0.078}\cdot 0.8H_2O$
$Mg_3AlBPTC$ (71%)	2.8	$Mg_{0.74}Al_{0.26}(OH)_2(BPTC)_{0.116}(Cl)_{0.047}\cdot 1.0H_2O$
$Mg_3AlBPTC$ (84%)	2.6	$Mg_{0.72}Al_{0.27}(OH)_2(BPTC)_{0.114}(Cl)_{0.022}\cdot 0.9\ H_2O$
$Mg_3AlBPTC$ (98%)	2.7	$Mg_{0.73}Al_{0.27}(OH)_2(BPTC)_{0.134}(Cl)_{0.003}\cdot 1.0H_2O$

for Mg_3Al-Bq, however, M^{II}/M^{III} molar ratios were equal to that of the precursors (Table S1). Furthermore, the amount of Bq and BPTC exchanged reaches values near 96% and 98% of the ion-exchange capacity (IEC), respectively.

The PXRD patterns for all of the samples are typical of reasonably well-defined hydrotalcite-like compounds, assuming rhombohedral symmetry (polytype 3R).[48,49] The (00*l*) basal reflections can be easily identified as a series of narrow, symmetric, equally spaced peaks at angles $2\theta < 30°$. It is well known that incorporation of bulk anions in the interlayer space of LDHs sometimes produce a strong turbostratic disorder, thus leading to broad, asymmetric reflections above ca. $2\theta \geq 30°$, and the turbostratic effect can be induced by the weak bonding interactions between the interlayer species and the host lattices. Many organic-anion-pillared LDHs exhibit this turbostratic structural feature.[47,50] In our case, encapsulation of Bq does not give rise to noticeable changes in the shape of the maxima recorded, suggesting a rather good ordering stack of the layers along the *c* axis (Figure 3). These results are similar to those previously reported by Arco et al. upon intercalation of $[Cr(C_2O_4)_3]^{3-}$ in the interlayer of a Mg−Al hydrotalcite.[51] As for $Mg_3Al-BPTC$, however, only a few loadings of BPTC do not give rise to important changes in the shape of the maxima recorded. When increasing the loading, increased turbostratic disorders are observed, i.e., the *hkl* reflections are order and less intense, and in fact several are not observed, as shown in Figures 1 and S1.

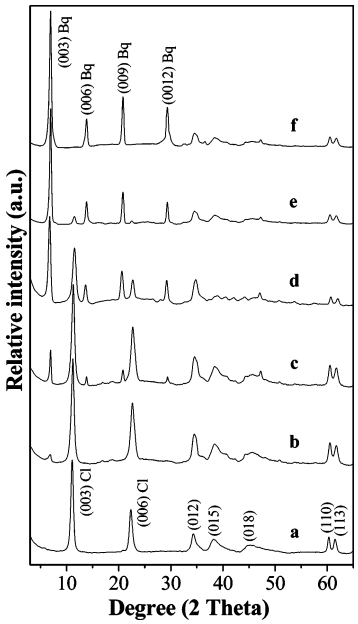

Figure 3. PXRD patterns for the Mg_3Al-Bq samples with different loading: (a) 2%, (b) 9%, (c) 28%, (d) 60%, (e) 71%, (f) 84%.

Figure 3 exhibits PXRD patterns of the intercalates with increasing Bq content. Interestingly, when a trace amount of Bq (=2% of IEC) is adsorbed, the interlayer spacing (7.90 Å) (Figure 3a) does not involve appreciable changes, compared with 7.95 Å of Mg_3Al-Cl (Figure 1a), and the surface uptake is near that expected from the BET surface area ($17\ m^2\cdot g^{-1}$). Additionally, the characteristic peak of Bq is observed in the excitation and emission spectra (see below). These indicate that Bq anions can be adsorbed on the external surface of the LDHs. What is noteworthy is that the basal reflection exhibits a strong shift to large *d* values when larger amounts of Bq are introduced into the LDHs, and the products contain two phases that have the basal spacings, 12.65 Å corresponding to the Mg_3Al-Bq and 7.90 Å corresponding to Mg_3Al-Cl, respectively, and the reflection peak at $d = 12.65$ Å is first weak, and the intensity of this reflection increases as the loading increases. Comparatively, the reflection peak at $d = 7.90$ Å decreases (Figure 3b−e). At 84% of IEC, only a phase with the basal spacing of 12.70 Å is obtained, and further loading of Bq does not give rise to appreciable modification of the PXRD patterns. The same phenomena from the patterns of $Mg_3Al-BPTC$ with increasing BPTC content, accompanied with the basal spacing of 12.60 Å, are also observed (Figure S1). These results indicate that even a small amount of Bq or BPTC anions intercalated are able to determine the interlayer spacing of the LDHs and that the arrangement of these anions in the host gallery must be very stable, not consistent with the orientations of the other linear anions with the various interlayer distances based on the starting guest/host ratios.[47,52] This is further indication that two different chemical environments on the LDHs (i.e., adsorption on the external surface and intercalation in the interlayer, which have different effect on the optical properties, see below) are successfully realized on the basis of finely modifying the anions/LDHs ratios, in agreement with the result of methyl orange-containing hydrotalcite.[29] It is worthwhile to mention that no staging intermediates are observed, probably their arrangements in the interlayer provide the best interactions between the host layers and guest anions.

Furthermore, parameter *a*, representing the average intermetallic distance, can estimate the metallic composition

(48) Bookin, A. S.; Cherkashin, V. I.; Drits, V. *Clays Clay Miner.* **1993**, *41*, 558.
(49) Bookin, A. S.; Drits, V. *Clays Clay Miner.* **1993**, *41*, 551.
(50) Xu, Z. P.; Braterman, P. S.; Yu, K.; Xu, H. F.; Wang, Y. F.; Brinker, C. J. *Chem. Mater.* **2004**, *16*, 2750.
(51) Del Arco, M.; Gutierrez, S.; Martin, C.; Rives, V. *Inorg. Chem.* **2003**, *42*, 4232.
(52) Kooli, F.; Chisem, I. C.; Vucelic, M.; Jones, W. *Chem. Mater.* **1996**, *8*, 1969.

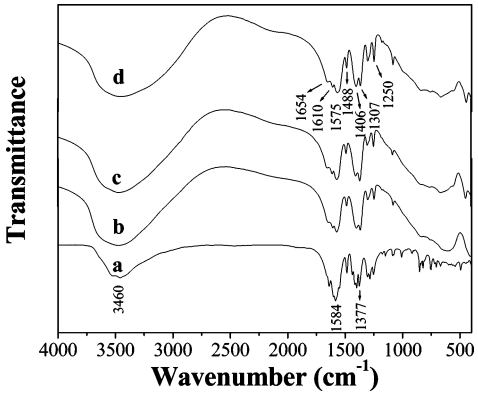

Figure 4. Fourier transform infrared spectra of (a) BPTC and the $Mg_3Al-BPTC$ samples with different loading: (b) 4%, (c) 38% (d) 85%.

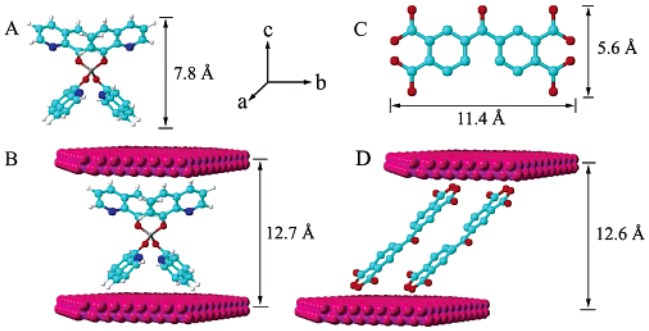

Figure 5. Molecule dimensions of free anions and schematic illustrations of the orientation of the intercalates.

because the greater the Al^{3+} amount in LDHs, the lower the mean metallic radius and the lower the mean intermetallic distance.[13,25] Table S2 shows parameter *a* values. However, it is worth noting that the *a* parameter for $Mg_3Al-BPTC$ decreases compared with that of the Mg_3Al-Cl precursor, confirming the partition dissolution of Mg^{2+} ions. These results are consistent with that of element analysis.

The hybrid materials ($Mg_3Al-BPTC$) display the common IR characteristics, as shown in Figure 4. The strong absorption bands at 1575 and 1370 cm^{-1} can be ascribed to the asymmetric and symmetric stretching vibration, respectively, of the carboxylic groups; according to Nakamoto,[53] the value of $\Delta\nu = \nu_{as} - \nu_s$ gives information about the symmetry of the interaction between the carboxylate groups and the hydroxylated layers. With $\Delta\nu$ values (200 cm^{-1}) of $Mg_3Al-BPTC$ similar to that (207 cm^{-1}) of the sodium salts, it seems to be possible to bridge both oxygen ions of the carboxylate to the layer hydroxyls. Whereas the strong absorption bands at 1654 and 1250 cm^{-1} are characteristic of the C═O and C−O vibrations, those at 1610, 1488, and 1406 cm^{-1} are attributed to the characteristic peaks of the benzene ring. All the peaks clearly show that the intercalation reactions are accomplished without any degradation of the BPTC molecule. The broad absorption band around 3460 cm^{-1} is due to the stretching of the hydroxyl groups (from the layers and the water molecules), which experiences a shift to lower wavenumber compared with the O−H stretch in free water at 3600 cm^{-1}.[53,54] This may be due to the formation of hydrogen bonding between the interlayer water and guest anions, as well as the hydroxyl groups of the host layers. In the low-frequency region, the bands at 660 and 447 cm^{-1} are attributed to the lattice vibration of M−O and M−O−M (M = Mg, Al) in the matrixes.

Anion Packing. As for the Bq fully exchanged example with the basal spacing 12.70 Å, the gallery height is close to 8.00 Å when subtracting the thickness of the host layer, 4.70 Å, from the corresponding basal spacing (d_{003}) value. This value is coincident with the height of the Bq anion (7.80 Å); that is, the anion should be arranged with the C2 axis perpendicular to the brucite-like layers (Figure 5B), which would considerably belong to the formation of a complicate aggregate (see below: the blue-shift and the fluorescence enhancement are not responsible for the formation of H- or J-aggregates). Probably, this orientation permits a maximum interaction between Bq and the layer of the host. Furthermore, Meyn et al.[55] pointed out that the interlamellar arrangement depends strongly on the area available to each interlayer anion in the host. Also, the guest orientation can reliably be explained by considering the dimension the Bq. The area per unit charge of the host lattice can be calculated from $(a^2 \sin 60)/x$, where *a* is the lattice parameter, *x* is the molar ratio of trivalent to total cations: 32 $Å^2$ for Mg_3Al-Bq. From the dimension of Bq, the cross-section area perpendicular to the C2 axis is about 30 $Å^2$, which is compatible with the area per unit charge for LDHs. So, the Bq anions might be arranged in such a way that they interact.

As for $Mg_3Al-BPTC$ with the basal spacing of 12.60 Å, the gallery height is close to 7.90 Å. Because the long axis length of BPTC anions is about 11.40 Å (Figure 5C), the BPTC anion should adopt a tilting longitudinal orientation at ca. 45°, similar to the tilting habit in saturated fatty acid intercalates (~60°),[56] as shown in Figure 5D. This arrangement fashion can be suitable for the stacking of large π systems and correspond to a J-type aggregate of dyes. According to the orientation analysis above, the area occupied by each BPTC anion in the *ab* plane is equal to about 50 $Å^2$. The area per unit charge of $Mg_3Al-BPTC$ is 30 $Å^2$. Hence, the area available per divalent anion is approximately 60 $Å^2$, which is suitable for BPTC with a monolayer arrangement with the J-type aggregate.

Thermal Stability Analysis. Given that thermal behavior is also an important factor in the application of optical material as the devices, the thermal stability of compounds is investigated by using TGA and in situ PXRD.

As shown by the TGA curves of Mg_3Al-Bq (Figure 6), two steps with noticeable weight loss are involved. The first step is attributed to the removal of surface-adsorbed water and interlamellar water up to about 180 °C. Another in the 250−550 °C temperature range contains two simultaneous processes: the dehydroxylation of the host matrix and the

(53) Nakamono, K. *Infrared and Ranman Spectra of Inorganic and Coordination Compounds*, 5th ed.; Wiley and Sons: New York, 1997.
(54) Yuan, Q.; Wei, M.; Evans, D. G.; Duan, X. *J. Phys. Chem. B* **2004**, *108*, 12381.
(55) Meyn, M.; Beneke, K.; Lagaly, G. *Inorg. Chem.* **1990**, *29*, 5201.
(56) Xu, Z. P.; Braterman, P. S. Layered Double Hydroxides: Multiple Phases and Self-Assembly. In *Encyclopedia of Nanoscience and Nanotechnology*; Marcel Dekker: New York, 2003.

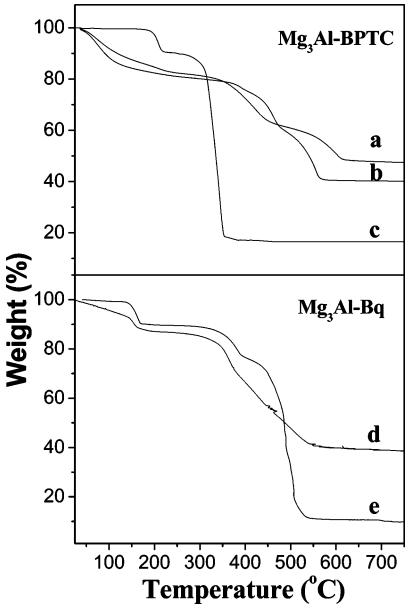

Figure 6. TGA curves for the intercalates: (a) $Mg_3Al-BPTC$ (38%), (b) $Mg_3Al-BPTC$ (85%), (c) the sodium salt of BPTC (d) Mg_3Al-Bq (9%), and (e) Mg_3Al-Bq (96%).

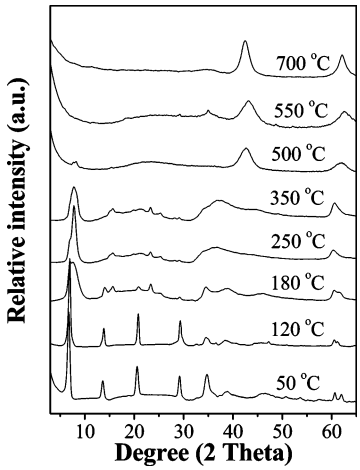

Figure 7. In situ PXRD patterns for the thermal decomposition of Mg_3Al-Bq (96%).

decomposition of Bq complexes. As for the TGA curves of $Mg_3Al-BPTC$ (Figure 6), however, we can observe the three steps with noticeable weight loss and the same first step with that of Mg_3Al-Bq. The second step, corresponding to the partial dehydroxylation of the host layers and decomposition of intercalated BPTC, extends from 250 to 450 °C. The third step, which takes place in the 470−600 °C range, can be attributed to the complete dehydroxylation of the host layers. These results indicate that these anions probably enhances the thermal stability of the host matrix compared with carbonate[57] and LDHs host also enhances the thermal stability of Bq and BPTC.

To identify the mechanism of the decomposition of the intercalate, PXRD diagrams of Mg_3Al-Bq (96%) calcined in air at increasing temperature in the range of 50−700 °C are shown in Figure 7. It can be observed that the basal reflection exhibits a shift to higher-angle 2θ with increasing

(57) Miyata, S. *Clays Clay Miner.* **1983**, *31*, 305.

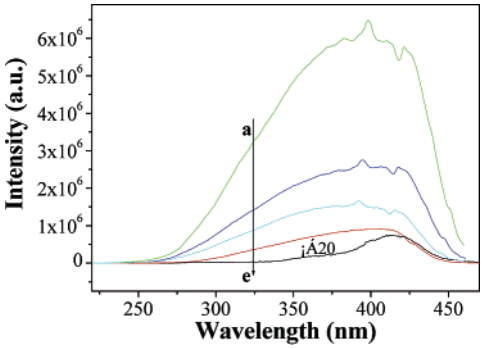

Figure 8. Excitation spectra of the Mg_3Al-Bq samples with different loading: (a) 9%, (b) 28%, (c) 84%, (d) 2%. (e) The spectrum of the dilute Bq/water solution (1.0×10^{-5} mol L^{-1}).

the temperature and that the decrease (1.90 Å) of the d_{003} values from 50 to 180 °C is related to the deintercalation of interlayer water molecules. The (003) and (006) diffraction peaks broaden and weaken remarkably at 250−350 °C, which possibly corresponds to the disordered structure as a result of the loss of the interlayer water and the decomposition of the intercalated Bq anions. However, the (110) diffraction peak close to 1.52 Å remains in the same position up to 350 °C, indicating that these materials are still lamellar. All the peaks associated with the LDHs disappear up to 550 °C. This is related to the decomposition of intercalated Bq and dehydroxylation of LDHs layers. The layer structure collapses completely at 550 °C with the first appearance of reflection from a cubic MgO phase at about 35.0°, 43.1°, and 62.6°, in agreement with that observed for the calcination of $Mg-Al-CO_3$.[57] The diffraction peaks of MgO become stronger as the temperature increases from 500 to 700 °C.

Fluorescence Properties Study. Figure 8 displays the fluorescence excitation spectra of Bq intercalated into LDHs. For comparison, the spectrum of dilute Bq/ethanol solution (1.0×10^{-5} mol·L^{-1}), which has a peak at 412 nm, is also shown in Figure 8e. The sample with very low loading has an excitation spectrum similar to that observed in a diluted solution of Bq, confirming that the Bq is bound to the host matrix mainly in monoanionic form and has negligible interaction with the neighboring molecules. This microenvironment is similar to that in the dilute water solution. Notably, increasing the loading of the Bq, the main excitation band at 399 nm progressively shifts to lower wavelengths. At the same time, a new excitation peak as compared to the monomeric excitation appears at ca. 421 nm, linked with the original band at 399 nm, and this new peak undergoes a slight blue-shift to the higher-energy side with increasing the Bq loading. However, with increasing the concentration of Bq solution, the excitation spectra were very similar except the change of the intensity. It is proposed that the new peak and the blue-shift may potentially due to the constrained geometry of the host and the arrangement of Bq in the interlayer (Figure 5B), as well as the increased intermolecular interaction between adjacent Bq molecules.

Figure 9 shows the fluorescence excitation spectra of $Mg_3Al-BPTC$ as a function of BPTC loading and of the dilute Bq/ethanol solution (1.0×10^{-5} mol·L^{-1}). The dilute solution shows only a broad peak in the region of 395−432

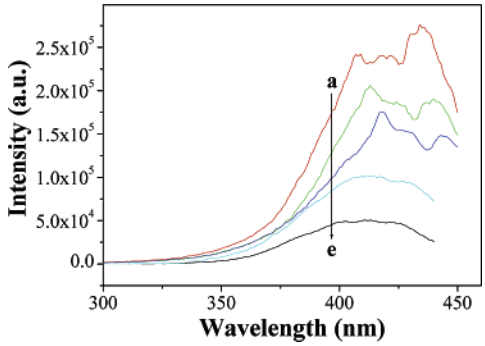

Figure 9. Excitation spectra of the $Mg_3Al-BPTC$ samples with different loading: (a) 12%, (b) 38%, (c) 85%, (d) 4%. (e) The spectrum of the dilute BPTC/water solution (1.0×10^{-5} mol L^{-1}).

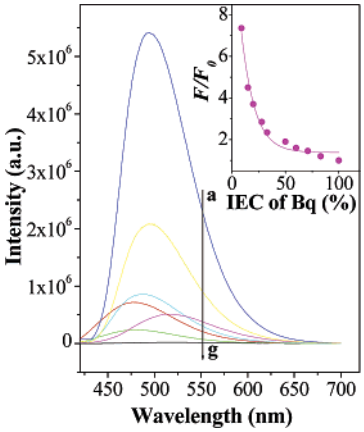

Figure 10. Emission spectra of the Mg_3Al-Bq for different loading (curves a−d) 9%, 28%, 2%, 84%, respectively, and (e) the pure Bq microcrystal, (f) the mixture with the host and Bq (15%), (g) in ethanol solution (1.0×10^{-5} mol L^{-1}). Inset: Fluorescence enhancement, F/F_0, of Bq as a function of its content intercalated.

nm. At very low loading of BPTC, the excitation spectra of $Mg_3Al-BPTC$ show changes similar to that of Mg_3Al-Bq. Upon the loading of the BPTC increasing, however, reverse shifts of the excitation maximum are observed compared with those of Mg_3Al-Bq, i.e., the main excitation band, centered at 434 nm, progressively shifts to higher wavelengths. Meanwhile, a new peak gradually appears at 408 nm and also shifts to the lower-energy side. It is obvious that these spectral changes are related to the constrained geometry of the host and the formation of BPTC J-aggregate in the exciton theory, which decreases the energy of the excited state,[58−60] although the presence of other types of aggregates cannot be excluded due to the nonplanar conformation of BPTC molecules. Furthermore, the relative intensity of the excitation band of the lower wavelengths over that of the high wavelengths gradually increases with the amount of BPTC on LDHs, which is attributed to the enhanced intermolecular interaction. This J-aggregate phenomenon is also verified in the absorption spectra (Figure S2). In addition, the excitation bands of Bq and BPTC molecules intercalated into LDHs are wider than those in the dilute solution. This is a general observation of dyes in solid-state samples and is attributed to the strong electronic interaction between the aromatic π system of guest anions and the electron lone pair of surface O atoms of the host layers.[58]

To further clarify the effects of the various aggregates of guests and the increased intermolecular interaction on the photophysical properties and discuss their effect on the fluorescence intensity, we recorded the fluorescence emission spectra of Mg_3Al-Bq and $Mg_3Al-BPTC$, as shown in Figure 10 and Figure S2, respectively. The emission spectrum of pure Bq solid crystals represents the characteristics of quinoline ligand band at 476 nm, assigned to $\pi^*-\pi$ transition (Figure 10e). Interestingly, the fluorescence maximum of Bq in ethanol ($\lambda_{max} = 516$ nm) undergoes a pronounced bathochromic shift about 40 nm, and the fluorescence intensity drastically decreases. This can mainly be attributed to solvent thermal quenching, whereas the spectra of the Bq incorporated in the host matrix are located between that of the solution and of the crystals. The sample with very low loading (2%) shows the same change with the excitation spectrum. Notably, the fluorescence intensity is much higher than that in diluted ethanol solution of Bq, indicating a reduction of the nonradiative deactivation process from the fluorescence excited state of Bq in rigid media. Increasing the loading of the Bq, the emission has a small shift of 10 nm, probably because of the increase in molecular interactions. When the loading is near the maximum value, the emission maximum, red-shifting about 9 nm in compared to that of the Bq microcrystal, seems to indicate that the distance between the Bq anions intercalated is larger than that in the crystal. These results are similar to those reported by Costantino et al.[29] The tunable fluorescence maximum is one of the factors to be considered in the development of new optical materials in the solid state. These results above indicate that the photophysical properties of guest molecules depend not only on the effect of the matrix (i.e., rigid, confined environment, etc), but also on the distribution and orientation of the Bq molecules on the host material, as well as on the guest−guest interactions.[6,7]

The Bq molecule is a rarely blue-emitting material, and this property is attributed to the combined effect of the electronic emission of quinoline ligand and the forceful conformation of rigid structure constructed by the B atom. Accordingly, if Bq molecules are rigidified, for instance by confinement in such limited spaces as the interlayers of LDHs, it could be expected that the fluorescence intensity be improved and controlled by the charge transfer between the intercalated guest molecules, which would be important to applications in devices and sensors. Here, we confirm that the fluorescence intensity of Bq intercalated significantly increases compared with that of pure Bq solid crystals, as shown in Figure 10. This increase in the fluorescence intensity is ascribed to the formation of host−guest supramolecular compounds by the electrostatic interaction. To further verify the fluorescence enhancement affected by the interaction of the host and guest and the confined environment of the host, the emission spectrum of the mixture with the host and the Bq microcrystal (15%) is detected and represents a

(58) Martínez, V. M.; Arbeloa, F. L.; Prieto, J. B.; Arbeloa, I. L. *J. Phys. Chem. B* **2005**, *109*, 7443.
(59) Fu, H.-B.; Yao, J.-N. *J. Am. Chem. Soc.* **2001**, *123*, 1434.
(60) An, B.-K.; Kwon, S.-K.; Jung, S.-D.; Park, S. Y. *J. Am. Chem. Soc.* **2002**, *124*, 14410.

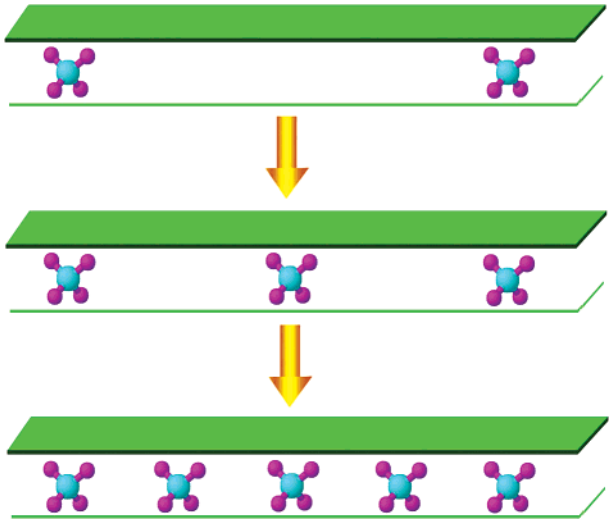

Figure 11. Schematic view of the interval between organic anions with an increase in the initial exchanged anions concentration.

decrease in intensity compared to the pure Bq solid (Figure 10f). Arbeloa and co-workers[58] also have demonstrated that a more rigid and constrained environment reduces the internal mobility and the flexibility of the quinoline system and increases the rigidity of guest molecule, decreasing the internal conversion processes and improving their fluorescence intensity. Here, the increased fluorescence intensity is quantified as the fluorescence enhancement, F/F_0: the ratio of the fluorescence intensity in the presence of LDHs to that in its absence. The dependence of the fluorescence enhancement on the Bq concentration intercalated is shown in the inset of Figure 10. The decrease of the fluorescence intensity with increasing Bq content is observed. Taking into account the change in the PXRD patterns (Figure 3) and the ideal model of the intercalation process (Figure 11), this can be explained: the interval between the Bq molecules in the host interlayer becomes increasing short with increasing Bq loadings, and Bq molecular motions are fairly constricted, increasing the nonradiative deactivation process from the fluorescent excited state of Bq. Consequently, the charge transfer between Bq molecules is enhanced and the fluorescence intensity reduced, i.e., the change can be attributed to the conventional concentration quenching.[61] In addition, Bq exhibits improved thermal stability up to about 350 °C, and its fluorescence intensity enhances with increasing temperatures mainly due to the effect of the co-intercalated water (Figure 12). The enhancement and controllability of the fluorescence intensity based upon the restrained geometry of the host and the guest−guest interaction create new opportunities for the use of these systems in the design of optical materials.

Except for the red-shift of emission maximum, the same phenomenon that the fluorescence intensity gradually decreases is also observed from the fluorescence spectra of Mg_3Al−BPTC with increasing BPTC loading (Figure S3), which can be attributed to the concentration quenching that the increased J-aggregate of the BPTC molecules caused. It is worth noting to mention that we observe a reversible color change of Mg_3Al−BPTC, that is, the high-loading samples

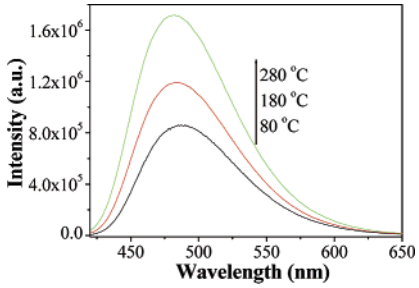

Figure 12. Emission spectra of the Mg_3Al−Bq after cooling the sample from various temperatures to room temperature under vaccum.

display green-blue color by X-ray irradiation and then recover to milk-white color with visible-light irradiation, which may be attributed to the photochromic behavior of BPTC on LDHs, whereas low-loading samples and pure BPTC microcrystal do not give rise to this photochromic phenomenon. Probably, the constrained geometry of the host and the increased guest−guest interaction would responsible for the photochemistry reaction of BPTC molecule in LDHs. However, the specific photochromic mechanism is not very clear and further investigation is in progress.

Conclusions

Two new photofunctional materials, Mg_3Al−Bq and Mg_3Al−BPTC, which represent the pure and well-crystallized products by the hydrothermal technique, have successfully been constructed with the ion-exchange approach, and Bq and BPTC molecules steadily arranged with C2 axis perpendicular to the layer plane and the J-type aggregation in the host interlayer, respectively. Compared with those of guests' monomer, the spectra of Mg_3Al−Bq and Mg_3Al−BPTC represent the reverse shift due to the various aggregates of the guests in the interlayer region and possess loading-tunability; that is, the bands evolve to the high-energy side and the low-energy side with an increase in their loading, respectively, attributed to the increased intermolecular interaction. Furthermore, their fluorescence intensity can be finely controlled by varying the guest content due to the concentration quenching, and Mg_3Al−Bq exhibits enhanced solid-state blue luminescence due to a more rigid and constrained environment of the host. This work presents a successful paradigm for finely modulating the optical properties of the photofunctional materials simply by changing the aggregates and the loading of guests. The optical control might have important practical applications, such as in device or sensor technologies.

Acknowledgment. This work was financially supported by the National Natural Science Foundation of China (No. 20371011).

Supporting Information Available: Chemical composition data; basal spacings and cell parameters; and additional spectra. This material is available free of charge via the Internet at http://pubs.acs.org.

IC0519887

(61) Endo, T.; Nakada, N.; Sato, T.; Shimada, M. *J. Phys. Chem. Solids* **1988**, *49*, 1423.